Review of corrosion behavior in fusion reactor cooling systems

Haibo Liu[a]*, Yuanyu Wu[a], Frederic Dacquait[b], Takayuki Shimaoka[a], Simone Noce[c], Alberto Previti[c], Luigi Di Pace[d], Pierre Cortes[a], Jaap G Van Der Laan[a], Vincent Bel[a], Olivier Chenais[a], Paul Edwards[a]

[a] ITER Organization, Route de Vinon-sur-Verdon, F-13067 Saint-Paul Lez Durance, France
[b] CEA, DES, IRESNE, DTN, Cadarache, F-13108 Saint-Paul lez Durance, France
[c] ENEA, NUC Department, Via E. Fermi 45, 00044 Frascati, Rome, Italy
[d] RINA Consulting-Centro Sviluppo Materiali (CSM) S.p.A, 00128 Castel Romano (RM), Italy
*Email: haibo.liu@iter.org

22/09/2026

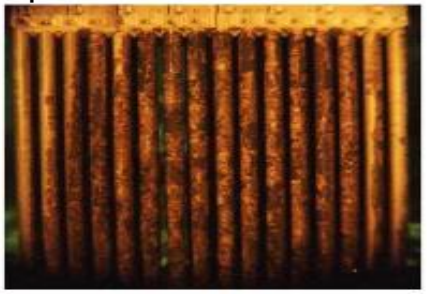
The views and opinions expressed herein do not necessarily reflect those of the ITER Organization

Content

- Introduction
- Corrosion
- Review of physical-chemical process impacting ACP
- Application of models and ACP prediction for ITER
- ACP knowledge acquisition
- Summary

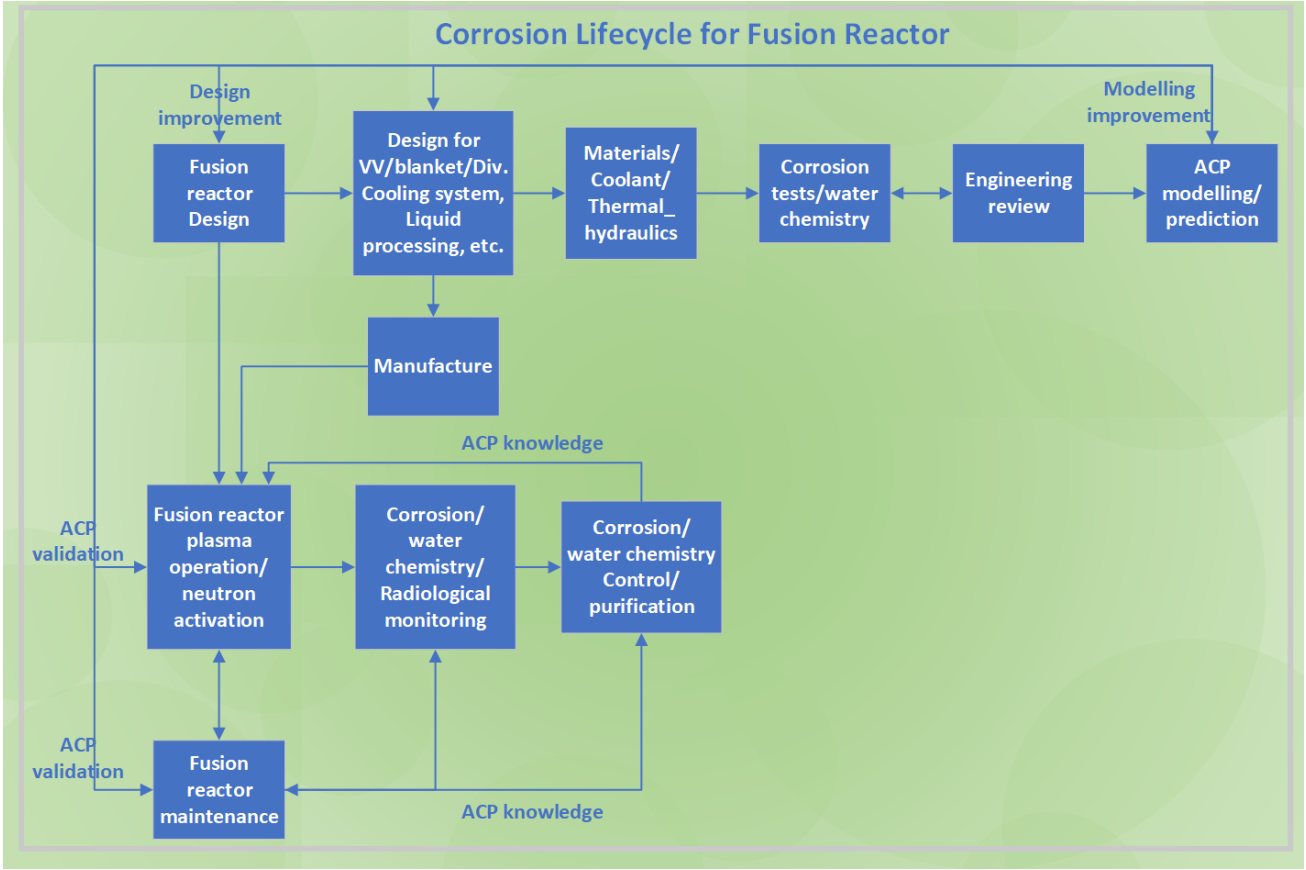
Introduction

- The fusion reactor will deposit hundreds/thousands of MW of fusion power on the vacuum vessel (VV), the components inside the VV and they need to be cooled by cooling system. The materials of the cooling system will face corrosion, which is defined as the chemical or electrochemical interaction between a material, usually a metal, and its environment. The corrosion products are activated in the neutron flux regions and transferred to the cooling loop.
- The corrosion behaviour and the activated corrosion product (ACP) contamination transfer could impact the structural integrity of the components, worker radiation exposure and radiological release consequence.
- Since for the ACP assessment, the main contribution is from the general corrosion (proceeding over whole metal wetted surface) process, this work gives a short review of the mechanisms of the general corrosion behaviour and what has been done in the previous years in order to improve the accuracy of the corrosion products prediction and its impact on the ITER ACP assessment.



Heavy CRUD deposition on fuel rods (see D. Walter, et al., November 2015 Annals of Nuclear Energy 85(6):1152-1166)

Introduction



The use of the new materials, like the CuCrZr alloy and reduced activation Ferritic/Martensitic steel (RAFM) under neutron flux regions, and the very different fusion reactor operating conditions, like the pulsed high energy fusion neutron, makes the corrosion behaviour in fusion reactor different from the one in fission reactor.

Corrosion

- In 2006 and 2008, Molander [1] and Jonas [2] did comprehensive review of the predicted corrosion and water chemistry aspects on the ITER water cooling systems: less favorable condition for water radiolysis suppression; copper alloy erosion; the need of reducing water condition to protect Cu-alloy from corrosion.

- **Reduced activation ferritic-martensitic steel**

The tested corrosion rates are from around one to several micron/year [4, 8-9]. The relatively low Cr content of RAFM steels may contribute to a higher corrosion rate and less protective oxide formation compared with higher-Cr content steels [8].

- **CuCrZr alloy**

CuCrZr alloy corrosion tests were performed by different parties under close to ITER and fusion DEMO reactor conditions. The tested corrosion rates range from less than one to hundreds of micron/year [3, 15-18].

These data remind the strong corrosion behaviour from CuCrZr if the water conditions cannot be controlled to a more favourable conditions.

On the other hand, during the ITER Start of Research Operation (SRO) and first Deuturium-Tritium (DT1) phase, because of the low neutron budget, the water radiolysis impact is not expected significant.

- **Semi-empirical correlations for CuCrZr corrosion rate**

Time power law based on Belous's test [3], Formula of Noce [21], etc.

Corrosion

- The components manufacture process could have impact on the cooling channels wetted surface quality and hence the corrosion behavior. The current blanket series production with CuCrZr wetted surface reduces the build-up of the unexpected oxide layer, bonded copper rich flakes and achieve surface roughness of < 1.6 µm [35-37].



Manufactured ITER blanket [36-37]

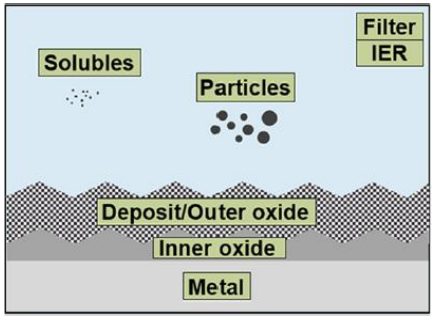


ITER Blanket CuCrZr high quality wetted surface [36-37]

Review of physical-chemical process impacting ACP

The process governing the formation of ACPs in a reactor water cooling system is complex and involves several interacting mechanisms. The following is the mechanisms modelled in OSCAR-Fusion v1.4 developed by CEA [25], which is currently used for ITER ACP prediction.

- Corrosion-release
- Erosion
- Deposition
- Dissolution-precipitation
- Advection/purification
- Neutron activation of materials
- Radioactive decay of ACP
- …



OSCAR v1.4 Media taken into account in the modelling

Several media are formed: deposit/outer oxide layer, inner oxide layer, ion, particle, filter/resin

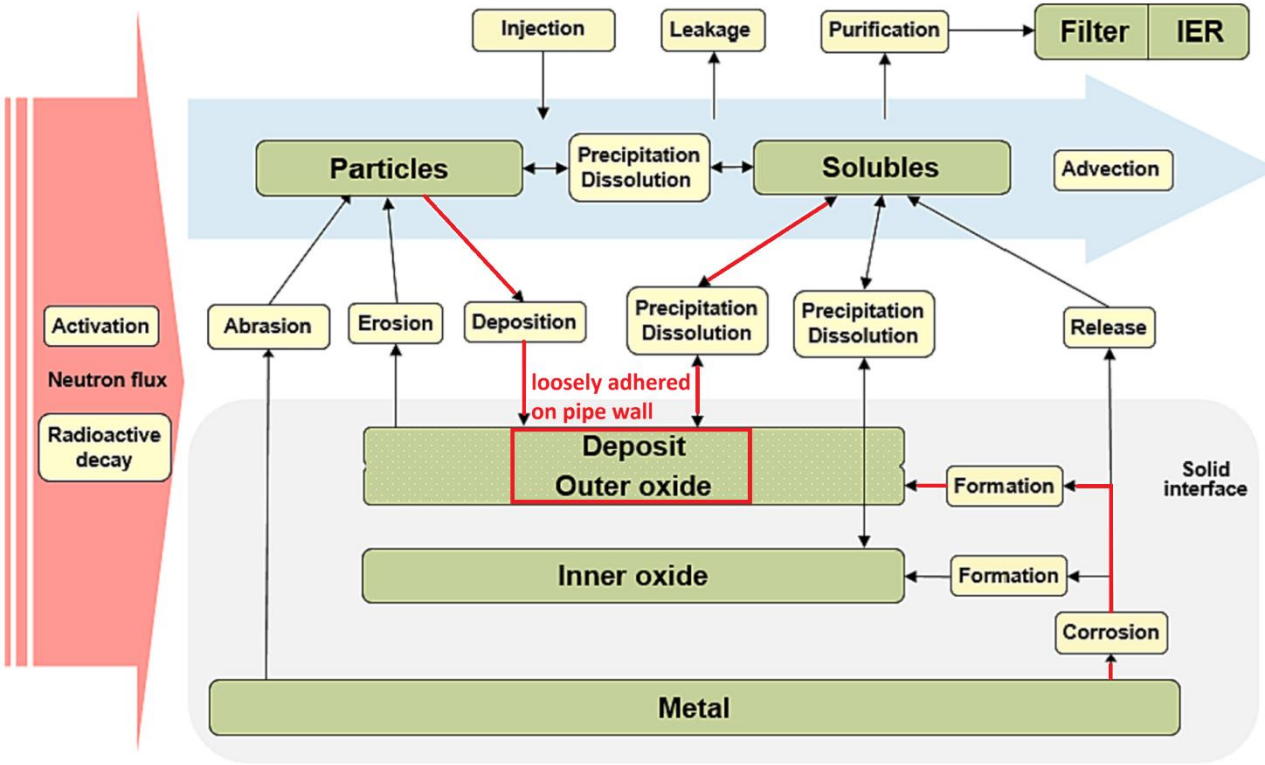
Deposit/outer oxide layer:

iron-rich layer (ferrite) for steel or copper oxide layer (Cu_2O/CuO) for copper alloy, which is loosely adhered to the wetted surface and could be mobilizable during abnormal coolant event.

Inner oxide layer: Cr-rich layer (chromite)

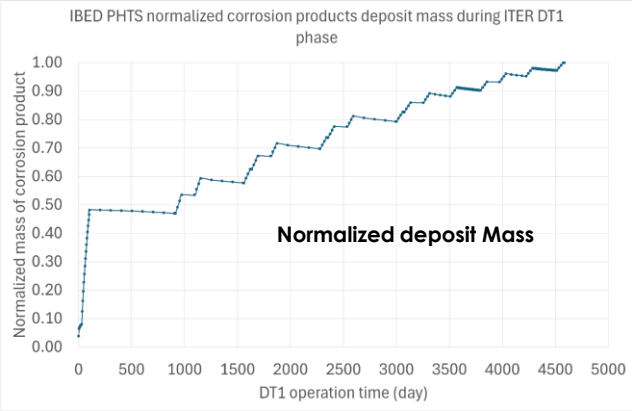
Review of physical-chemical process impacting ACP

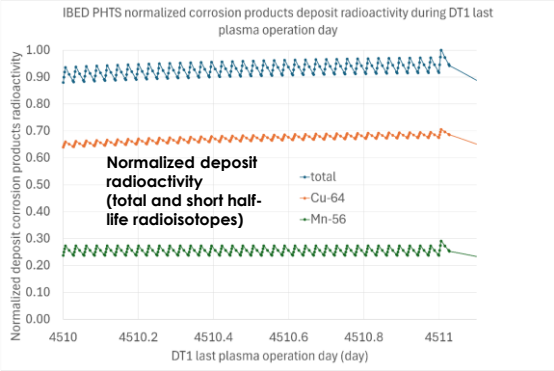
OSCAR-Fusion v1.4 mass transfer mechanisms [23]:

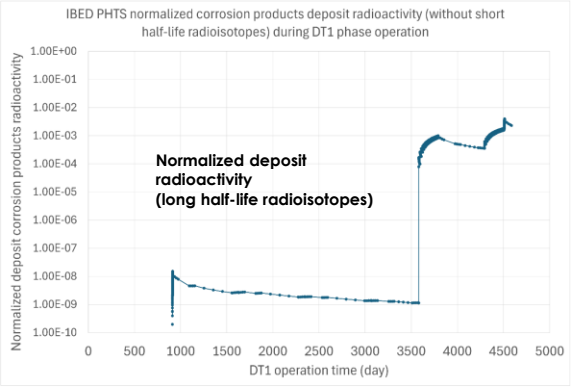


Application of models and ACP prediction for ITER

ITER IBED Primary Heat Transfer System (PHTS) normalized corrosion products deposit results







- Both the IBED ACP deposit mass and radioactivity are higher than the results from the assessment in 2000 [34].

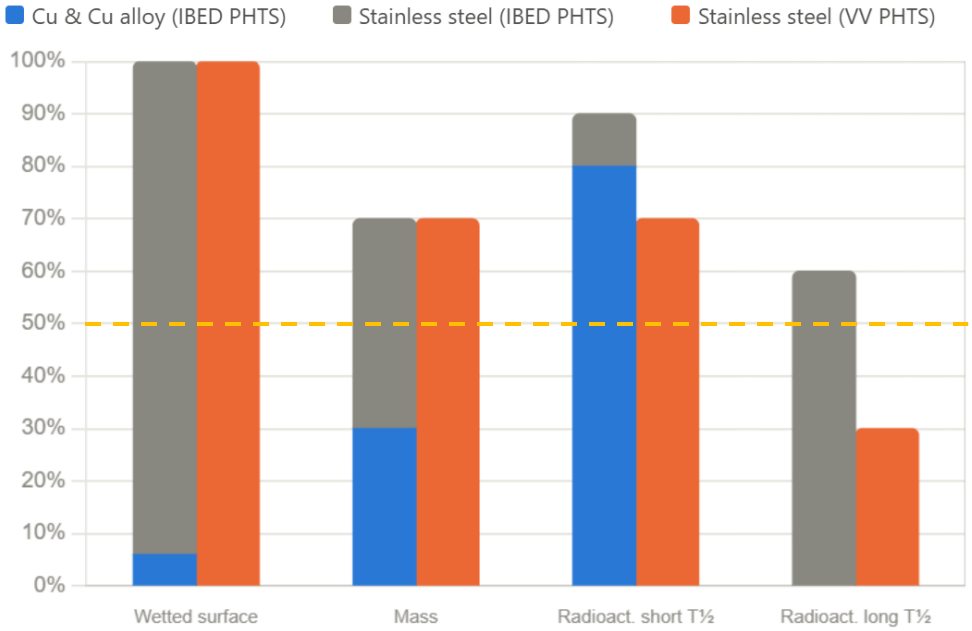
- **General observation:**

The short half-life radioisotopes activity oscillates during the simulated plasma pulses and it's the main contribution. This patten is true for the tokamak fusion reactor and the results mainly depend on the pulse length and fusion power.

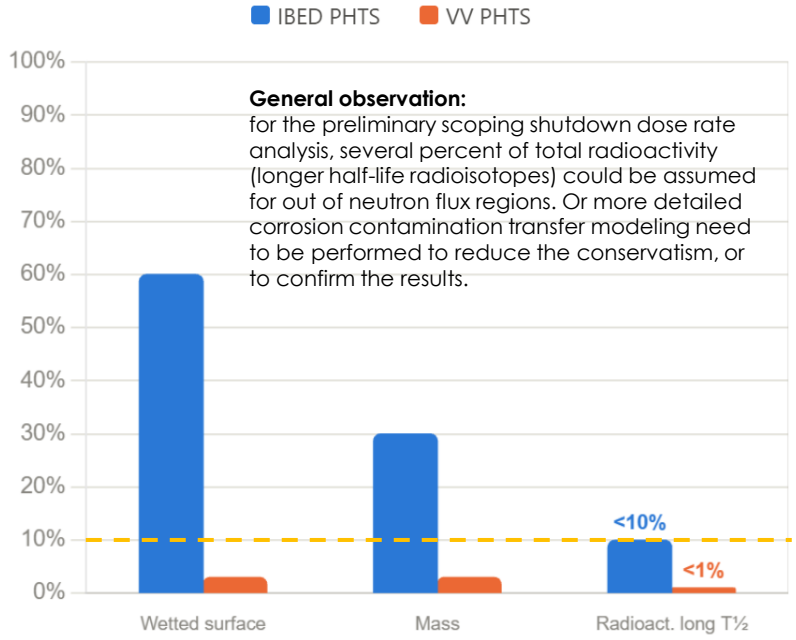
- **General observation:**

The neutron budget lumping may create over conservative ACP radioactivity. Simulating some plasma pulses at the end of operation scenario is the accurate way to obtain the radioactivity results for the very short half-life radioisotopes.

Application of models and ACP prediction for ITER



Mobilizable corrosion products deposit contribution (relevant to abnormal coolant event impact assessment)



Out of neutron flux regions corrosion products contribution (relevant to normal operation shutdown dose rate assessment)

ACP knowledge acquisition

- The ITER 2024 new baseline [29] defines the stepwise operation approach. The stepwise operation approach will provide the opportunity for the operator to learn and justify or improve the water chemistry control (through Chemical and Volume Control System) during the commissioning, SRO and DT1 phases. And the passivation process for the water cooling loops could be practiced during the earlier phases operation to understand the real wetted surface response to the water conditions.

- These earlier phases operation will provide guidance and reduce uncertainty for the later DT2 phase corrosion control strategies. The potential corrosion risks should be identified and managed during the earlier phases operation to avoid costly repairs at later operation phase, and to maintain the designed ITER facility performance and availability.

Summary

- **General observation:** the fusion reactor ACP radioactivity oscillates during the simulated plasma pulses, and the result depend mainly on the pulse length and fusion power.

- **General observation:** the fusion reactor ACP prediction shall model some plasma pulses at the end of the operation scenario to avoid any over-conservatism because of the neutron budget lumping.

- **General observation:** the fusion reactor ACP out of neutron flux regions radioactivity normally contributes several percent of total activity. If scoping analysis with this assumption produces high dose rate, more detailed corrosion contamination modeling need to be performed.

R&D priority for fusion reactor general corrosion study:

- More tests to verify the CuCrZr and RAFM corrosion and release rates under typical fusion reactor conditions are proposed. How to control and mitigate the materials corrosion in fusion environment, and how to make a passivation layer (layer of protection) for the new materials shall be investigated.

References

[1] Private communication, Anders Molander, Corrosion and water chemistry aspects concerning the tokamak cooling water systems of ITER, Studsvik/N-06/186 TW5-TVM-LIP, 2006.
[2] Private communication, Otakar Jonas, Lee Machemer, Corrosion, Activation, Water chemistry, and materials – ITER Tokamak cooling water systems – interim assessment, Oak Ridge ITER task 4 report, June 2008.
[3] V. Belous, Assessment of the corrosion behaviour of structural materials in the water coolant of ITER, 258-263 (1998) 351-356, Journal of Nuclear Materials.
[4] E. Piccolo, et al., Preliminary Assessment of Cooling Water Chemistry for Fusion Power Plants, 2021, 2, 512-530, Corrosion and materials degradation.
[5] D. Tarabelli, Pactiter (Pactole version for ITER) – Final report, Note Technique DEC/SECA/LTC/98-150, CEA, 06/1998.
[6] D. Carloni, et al., Use of the OSCAR-Fusion V1.4.a code for a preliminary assessment of the ACP contamination within the main ITER water cooling circuit, 64 (2024) 076050, Nuclear Fusion.
[7] L. Giancarli, et al., The research plan for the ITER TBM program, 231 (2026) 115943, Fusion Engineering and Design.
[8] A. Kimura, et al., A. Kimura et alii "Ferritic steel-blanket systems integration R&D- Compatibility assessment, Fusion Engineering and Design 2006.
[9] M. Nakajima, et al., Corrosion Properties of F82H in Flowing High Temperature Pressurized Water, J. Plasma Fusion Res. SERIES, 11 (2015) 69
[10] J.H. You, et al., Fusion Eng. Des. 175 (2022) 113010
[11] M. Sardo, et al., EU ITER first wall panel CuCrZr material procurement and characterization, 222 (2026) 115417, Fusion Engineering and Design.
[12] Private communication, E. Piccolo, et al., Corrosion Tests for ACPs studies -Assessment of the corrosion behavior of CuCrZr material in the water coolant of ITER, P0042942-1-H1, 2025.
[13] J. Zheng, et al., Erosion–corrosion tests on ITER copper alloys in high temperature water circuit with incident heat flux, volume 61-62, 649-657, 2002, Fusion Engineering and Design.
[14] E. Tevissen, et al., CuCrZr release rate evaluation in ITER operating conditions, NT DEN/DTN/STM/LMTR/2007-27 ind. 0 du 25/11/07.
[15] Y. Huang, et al., The effect of dissolved oxygen respectively dissolved hydrogen on corrosion behavior of CuCrZr alloy in high temperature water, volume 31, 101190, 2022, Nuclear Materials and Energy.
[16] Y. Huang, et al., Corrosion and stress corrosion behavior of CuCrZr alloy in high temperature pure water environment relevant to Japan's DEMO divertor, volume 202, 114364, 2024, Fusion Engineering and Design.
[17] Johan Oijerholm, et al., Assessment of flow-assisted corrosion rate of copper alloy cooling tube for application in fusion reactors, Nuclear Materials and Energy 35 (2023) 101433.
[18] C. Obitz, et al., Erosion corrosion of CuCrZr specimens expose d for simulated ITER operational conditions, 000 (2016) 1-6, Nuclear Materials and Energy.
[19] E. Lo Piccolo et al., "EFDA_D_2R8GE3 v1.2 - PrIO-5.2.2-T004-D001-Report on measurements of erosion/corrosion on ITER material samples (CuCrZr) in baking conditions_ENEA", 2023
[20] E. Tevissen and Y. Philbert. (2009), Measurement of copper release in CORELE loop under reducing conditions, technical report CEA/DEN/DTN/SMTM/LMTR/2009/37/0.
[21] S. Noce, et al., Neutronics, radiolysis and OSCAR-Fusion analysis for the design of a flow loop for Activated Corrosion Products studies, 231, 115911, 2026, Fusion Engineering and Design.
[22] S. Noce, et al., OSCAR-Fusion analysis of the first Copper dust campaign in the FNG ACP hydraulic loop, 34th Symposium on Fusion Technology, 2026.
[23] BROUTIN Francois, DACQUAIT Frédéric, OSCAR Fusion v1.3, DESCRIPTION OF THE PHYSICAL MODELS, CEA/DEN/CAD/DTN/SMTA/LMTR/NT/2016-21-VERSION A
[24] S.E. Ziemniak and M. Hanson, Corrosion behavior of 304 stainless steel in high temperature, hydrogenated water, Corrosion Science 44 (2002) 2209-2230
[25] F. Dacquait, et al., Simulation of Co-60 uptake on stainless steel and alloy 690 using the OSCAR v1.4 code integrating an advanced dissolution-precipitation model, 405 (2023) 112190, Nuclear Engineering and Design.
[26] F. Dacquait, et al., Modelling of the contamination transfer in nuclear reactors: The OSCAR code - Applications to SFR and ITER. Challenges for Coolants in Fast Neutron Spectrum Systems. 5-7 July 2017, Vienna (Austria), IAEA, IAEA-TECDOC-1912, 77-83 (2017).
[27] D. Macdonald, et al., A Critical Review of Radiolysis Issues in Water-Cooled Fission and Fusion Reactors: Part I, Assessment of Radiolysis Models, Corrosion and materials degradation, 2022, 3, 470-535.
[28] D. Macdonald, et al., A Critical Review of Radiolysis Issues in Water-Cooled Fission and Fusion Reactors: Part II, Prediction of Corrosion Damage in Operating Reactors, Corrosion and materials degradation, 2022, 3, 694-758.
[29] P. Barabaschi, et al., ITER progresses into new baseline, 215 (2025) 114990, Fusion Engineering and Design.
[30] Private communication, H. Liu, DT1 IBED loop Activated Corrosion Products assessment, 2026.
[31] Private communication, H. Liu, DT1 VV PHTS loop activated corrosion products assessment, 2026.
[32] Private communication, V. Bel, Safety irradiation scenario.
[33] Private communication, Blanket NHF first all panels without steel liner, 2020.
[34] L. DI PACE, et al., ACTIVATED CORROSION PRODUCTS EVALUATION FOR THE ITER TCWS, FUS TN SIC TR 11/00, 2000.
[35] Private communication, Drilling Demonstration Plan, ITER 2021.
[36] R. Shuff, et al., ITER NHF First Wall Full Scale Prototype manufacturing and testing, 220 (2025) 115317, Fusion Engineering and Design.
[37] Private communication, Hot Evacuation HIP Procedure, ITER 2025.

Thank you very much

Application of models and ACP prediction for ITER

Mode	Duration [days]	Comment
Commissioning		
Dwell during System /integrated commissioning	30	to simulate the system/integrated commissioning period
Baking during Integrated Commissioning	74	2 months + 2 weeks
SRO (27 months SRO + 8 months LTM)		
Dwell	807	27 months
Plasma session	30 pulses during 3 days	
Baking	60	baking after SRO for H&D removal
Cold-shutdown	120	
Baking	60	baking before FPO for wall conditioning
FPO1-3 (6 years, assuming 0 power)		
FPO4 (16 months FPO (~ 0.68 day 500 MW) + 8 months LTM)		
Dwell	196	First 8 months
Baking	60	baking during FPO for wall conditioning
Dwell	10.9572 x (16 sessions)	during second 8 months
Plasma session	0.0428 x (16 sessions)	during second 8 months
Short Term Maintenance	3 x (16 sessions)	during second 8 months
Baking	60	baking after FPO for tritium removal
Cold-shutdown	120	
Baking	60	baking before FPO to remove impurities
FPO5 (16 months (~ 1.6 days 500 MW) + 12 days cooling)		
Dwell	190	first 8 months
Baking	60	baking during FPO for wall conditioning
Dwell	10.9395 x (16 sessions)	during second 8 months
Plasma session	0.0605 x (16 sessions)	during second 8 months
Short Term Maintenance	3 x (16 sessions)	during second 8 months
Plasma session	36 pulses per day + 1 pulse 700 MW	
Short Term Maintenance	3	STM (condition as dwell)
Baking	60	baking after FPO for tritium removal
Cold-shutdown	12	

Modelled SRO and DT1 operation scenario (~ 12 years)

Application of models and predictions for ITER

The ACP inventories in the ITER IBED PHTS, VV PHTS and NBI PHTS are currently modelled with the OSCAR v1.4 code [30-31].

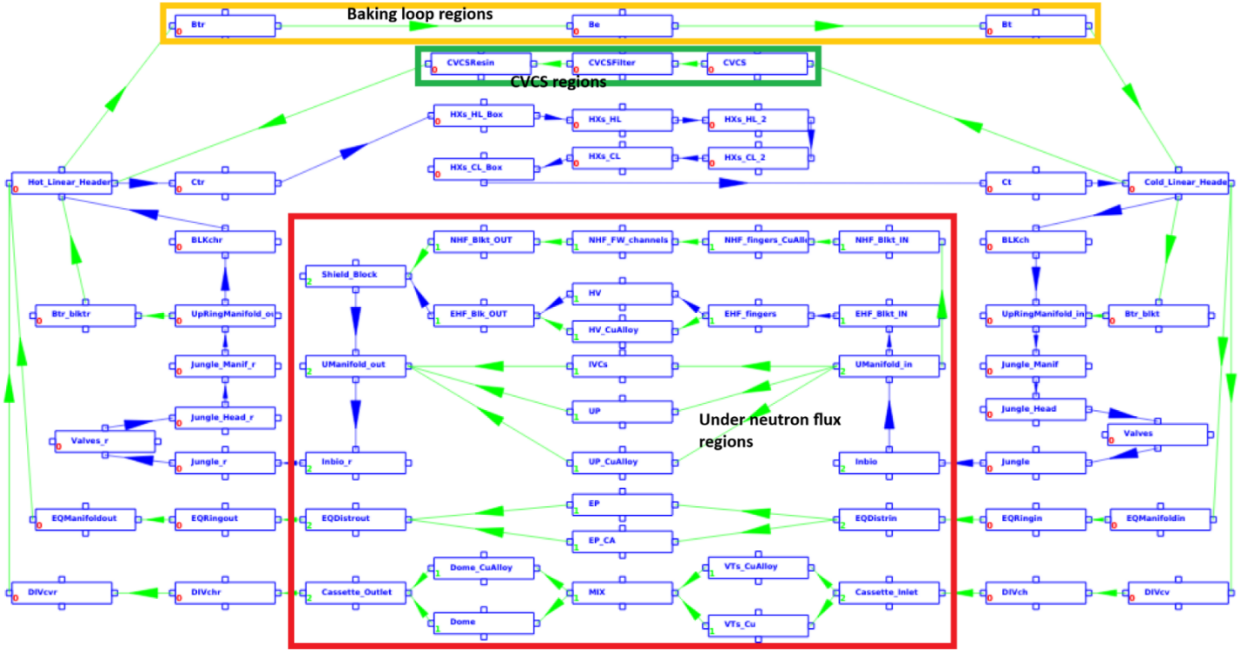


Figure: IBED PHTS nodalization diagram in OSCAR-Fusion

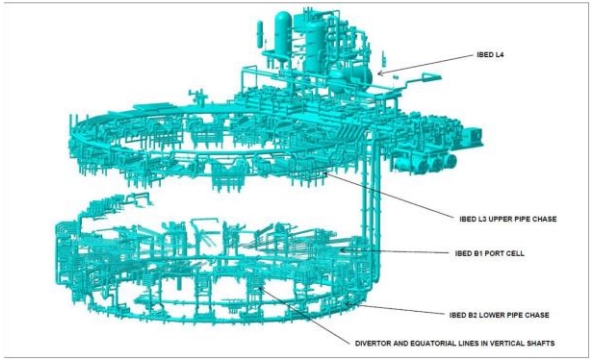


Figure: ITER IBED PHTS 3D model

Application of models and predictions for ITER

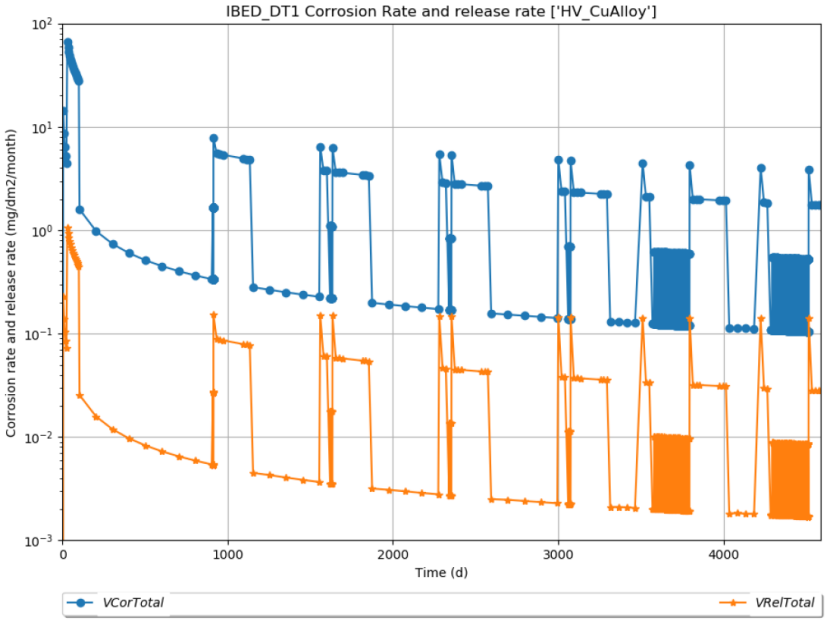


Figure: CuCrZr Corrosion rate and release rate in IBED HV_CuAlloy region

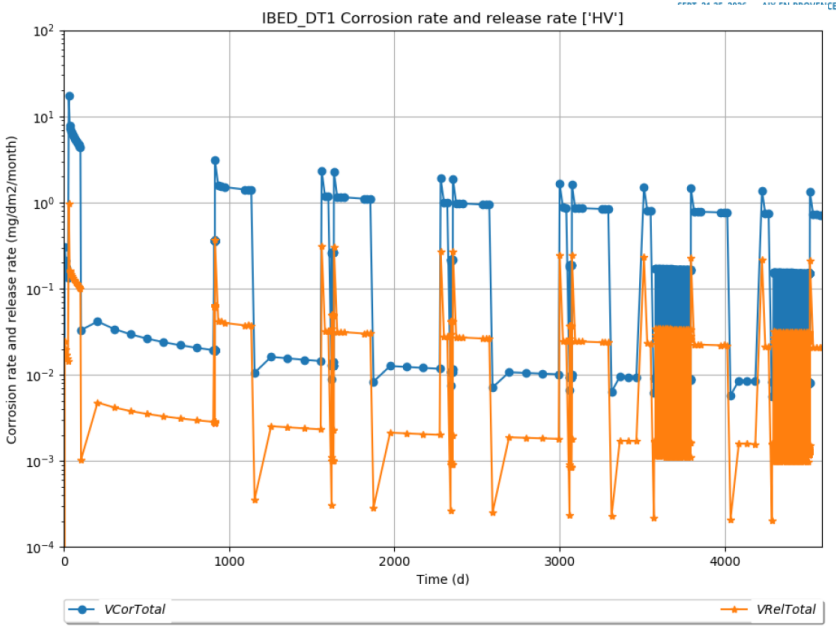


Figure: Stainless steel corrosion rate and release rate in IBED HV region

During IBED baking at 220 ^{o}C, it has corrosion rate of several to ten micron/year for CuCrZr and ~ 1 micron/year for stainless steel.

Application of models and predictions for ITER

ITER irradiation scenario, thermal hydraulic parameters and materials composition

Table 3: ITER SRO and DT1 irradiation scenario [32]

Campaign	Duration [year]	Plasma species	Neutron yield ($x10^{24}$) [n]	Duration assuming 500 MW DT power [days]
SRO	27 months	DD	0.00015	9.78E-06
FPO-1	2	-	0	0
FPO-2	2	-	0	0
FPO-3	2	-	0	0
FPO-4	2	DT	10.5	0.684
FPO-5	2	DT	24.5	1.598

The operation scenario has the last day with plasma pulses. And the other neutron budget is lumped during 8 months of each 2 years fusion power operation.

Table4: IBED PHTS thermal-hydraulic parameters during ITER different operational phases

Phase	Coolant Temperature [°C]	Flow Rate [kg/s]	Coolant Pressure [bar]	Power Fraction
SRO				
Dwell	80	4821	40	0
Baking	225	483	44	0
FPO				
Burn	141 (hot leg) 80 (cold leg)	4821	40	1
Dwell	80	4821	40	0
Baking	225	483	44	0

Table6: VV PHTS thermal-hydraulic parameters during ITER different operational phases

Phase	Coolant Temperature [°C]	Flow Rate [kg/s]	Coolant Pressure [bar]	Power Fraction
SRO				
Dwell	117	1000	8	0
Baking	185	500	18	0
FPO				
Burn	117 (cold leg)	1000	8	1
Dwell	117	1000	8	0
Baking	185	500	18	0

Table 5: Material composition and properties used in IBED PHTS model

Material name	AISI316_ 12 mic	AISI316_ 6 mic	AISI316_ 2 mic	AISI316_ 12 mic20	Cu alloy	Cu
Composition	Co 0.0005 Cr 0.175 Cu 0.003 Fe 0.648 Mn 0.018 Ni 0.123	Co 0.0005 Cr 0.175 Cu 0.003 Fe 0.648 Mn 0.018 Ni 0.123	Co 0.0005 Cr 0.175 Cu 0.003 Fe 0.648 Mn 0.018 Ni 0.123	Co 0.002 Cr 0.175 Cu 0.003 Fe 0.648 Mn 0.018 Ni 0.123	Co 0.0005 Cr 0.0075 Cu 0.99148 Fe 0.0002 Mn 2e-05 Ni 0.0003	Co 0.0005 Cr 0.0001 Cu 0.9991 Fe 0.0001 Mn 0.0001 Ni 0.0001
Roughness	12 µm	6 µm	2 µm	12 µm	1.6 µm	6.3 µm
Regions	Out-of-flux and in-flux regions	DIV stainless steel parts	HXs	Isolation Valves	In-flux regions	IVCs Divertor swirl tubes

Table 7: Material composition and properties used in VV PHTS model

Material name	AISI316_12 mic	AISI316_2 mic	AISI304B7
Composition	Co 0.0005 Cr 0.175 Fe 0.648 Mn 0.018 Ni 0.123	Co 0.0005 Cr 0.175 Fe 0.648 Mn 0.018 Ni 0.123	Co 0.0005 Cr 0.19 Fe 0.6495 Mn 0.02 Ni 0.14
Roughness	12 µm	2 µm	12 µm
Regions	other regions	part of HXs	VV region and its extension

Application of models and predictions for ITER

Radioisotopes and reaction rates

Table 1. Radioisotopes considered in OSCAR

Isotope	Gamma emitter	Half life
Co57	Yes	271.8 d
Co58	Yes	70.8 d
Co60	Yes	5.27 y
Cr51	Yes	27.7 d
Cu62	Yes	585 s
Cu64	Yes	12.7 h
Cu66	Yes	306 s
Fe55	No (X ray)	2.68 y
Fe59	Yes	44.5 d
Mn54	Yes	312 d
Mn56	Yes	2.58 h
Ni57	Yes	1.5 d
Ni59	No (X ray)	76040 y
Ni63	No	100 y

Table 2. Details of nuclear reaction rates

Reaction/s location	BM15 FW	BM15 SB
Co59(n,gamma)Co60	7.75E-10	5.25E-10
Cr50(n,gamma)Cr51	2.23E-10	1.53E-10
Cr52(n,2n)Cr51	5.10E-12	1.46E-12
Fe54(n,gamma)Fe55	3.35E-11	2.29E-11
Fe54(n,p)Mn54	1.01E-11	3.43E-12
Fe56(n,2n)Fe55	8.60E-12	2.52E-12
Fe56(n,p)Mn56	2.48E-12	7.60E-13
Fe58(n,gamma)Fe59	2.20E-11	1.50E-11
Mn55(n,2n)Mn54	1.42E-11	4.19E-12
Mn55(n,gamma)Mn56	2.21E-10	1.51E-10
Ni58(n,2n)Ni57	4.43E-13	1.27E-13
Ni58(n,alpha)Fe55	2.45E-12	7.80E-13
Ni58(n,d)Co57	1.75E-11	3.44E-12
Ni58(n,gamma)Ni59	6.75E-11	4.63E-11
Ni58(n,p)Co58	1.14E-11	3.96E-12
Ni60(n,p)Co60	3.31E-12	1.03E-12
Ni62(n,gamma)Ni63	2.07E-10	1.42E-10
Cu63(n,alpha)Co60	1.01E-12	3.11E-13
Cu63(n,gamma)Cu64	7.80E-11	5.30E-11
Cu65(n,2n)Cu64	1.79E-11	5.30E-12

Materials corrosion rate

- **CuCrZr alloy**

CuCrZr alloy corrosion tests were performed by different parties under close to ITER and fusion DEMO reactor conditions.

V. Belous, et al., Assessment of the corrosion behaviour of structural materials in the water coolant of ITER, 1998, Journal of Nuclear Materials [3].

Belous concluded the CuCrZr corrosion rate is close to time power law, and tested corrosion rate from less than 1 micron/year to several micron/year at reduced water condition.

C. Obitz, et al., Erosion corrosion of CuCrZr specimens expose d for simulated ITER operational conditions, 2016, Nuclear Materials and Energy [18].

Obitz's test shows that corrosion rates under alternating ECP conditions are approximately three times higher than those observed in continuously oxidized water and about thirty times higher than those measured in reduced water condition. And the corrosion rates could go to several tenths of micron/year under oxidizing condition and hundreds micron/year under 150 ^{o}C high velocity cyclic ECP condition. There is one observation that the erosion corrosion rate does not decrease with time.

Johan Oijerholm, et al., Assessment of flow-assisted corrosion rate of copper alloy cooling tube for application in fusion reactors, Nuclear Materials and Energy, 2023 [17].

Oijerholm observed low corrosion rate under hydrogenated, oxygen-free conditions. At the 150 ^{o}C oxidizing condition, the corrosion rate is also several tenths of micron/year. It also observed that the flow assisted corrosion rate is approximately linear with time across the examined exposure period.

Y. Huang, et al., The effect of dissolved oxygen respectively dissolved hydrogen on corrosion behavior of CuCrZr alloy in high temperature water, 2022, Nuclear Materials and Energy [15-16].

Huang observed highest weight loss under oxygenated condition

All these data remind the stronger corrosion behaviour from CuCrZr if the water condition cannot be controlled to a more favourable condition, compared with the behaviour of steel.

On the other hand, during the ITER Start of Research Operation (SRO) and Deuturium-Tritium-1 (DT1) phases, because of the low neutron budget, the water radiolysis impact is not expected significant, and the water chemistry could be achieved to favourable condition to control and mitigate water corrosion.

Application of models and predictions for ITER

Details of SRO and DT1 operation scenario (~ 12 years)

Mode	Duration [days]	Comment
Calculation Initialization		
Calculation initialization	1 [s]	calculation initialize
Commissioning		
Dwell during System /integrated commissioning	30	to simulate the system/integrated commissioning period
Baking during Integrated Commissioning	74	2 months + 2 weeks
SRO (27 months SRO + 8 months LTM)		
Dwell	807	27 months
Plasma session	4 pulses per day (1day) + 13 pulse per day (2 days)	3 days SRO 50 s per pulse operation
Baking	60	baking after SRO for H&D removal
Cold-shutdown	120	
Baking	60	baking before FPO for wall conditioning
FPO1-3 (16 months FPO (zero power) + 8 months LTM per FPO)		
Dwell	406	
Baking	60	baking during FPO for wall conditioning
Plasma session	11	0 fusion power with coolant T at plasma phase
Short Term Maintenance	3	STM (condition as dwell)
Baking	60	baking after FPO for tritium removal
Cold-shutdown	120	
Baking	60	baking before FPO for wall conditioning

FPO4 (16 months FPO (0.684 day 500 MW) + 8 months LTM)		
Dwell	196	First 8 months
Baking	60	baking during FPO for wall conditioning
Dwell	10.9572 x (16 sessions)	during second 8 months
Plasma session	0.0428 x (16 sessions)	during second 8 months
Short Term Maintenance	3 x (16 sessions)	during second 8 months
Baking	60	baking after FPO for tritium removal
Cold-shutdown	120	
Baking	60	baking before FPO to remove impurities
FPO5 (16 months (1.598 days 500 MW) + 12 days cooling)		
Dwell	190	first 8 months
Baking	60	baking during FPO for wall conditioning
Dwell	10.9395 x (16 sessions)	during second 8 months
Plasma session	0.0605 x (16 sessions)	during second 8 months
Short Term Maintenance	3 x (16 sessions)	during second 8 months
Plasma session	36 pulses per day + 1 pulse 700 MW	
Short Term Maintenance	3	STM (condition as dwell)
Baking	60	baking after FPO for tritium removal
Cold-shutdown	12	For FPO5, the shutdown is limited to 12 days

Application of models and predictions for ITER

Table 8. Wetted surface areas, CP medium mass and radioactivity contributions

Regions and CP medium	Properties	ITER IBED PHTS	ITER VV PHTS
Wetted surface			
Under neutron flux regions	wetted surface (m^2)	~ 10000	~ 21000
Out of neutron flux regions	wetted surface (m^2)	~ 15000	~ 1000
Cu and Cu alloy under neutron flux regions	wetted surface (m^2)	~ 1500	NA
Whole loop	wetted surface (m^2)	~ 25000	~ 22000
Out-of-flux/whole loop	wetted surface %	~ 60%	~ 3%
Cu&Cu alloy/whole loop	wetted surface %	~ 6%	NA
CP medium mass and radioactivity contribution			
Cu and Cu alloy total CP deposit/total	Mass %	~ 30%	NA
	Radioactivity with short half-life %	~ 80%	NA
CP deposit/total (relevant to mobilizable CP during abnormal coolant event)	Mass %	~ 70%	~ 70%
	Radioactivity with short half-life %	~ > 90%	~ 70%
	Radioactivity without short half-life %	~ 60%	~ 30%
% of CP total outflux/total (relevant to normal operation dose rate after shutdown)	Mass %	~ 30%	~ 3%
	Radioactivity without short half-life %	~ < 10%	~ < 1%

Observation 1: for the preliminary scoping shutdown dose rate analysis with basic material corrosion rate data and cooling system design, if it produces unacceptable dose rates values in the rooms with the assumption of several percent of total radioactivity (longer half-life radioisotopes), the assessment with more detailed corrosion contamination transfer modeling, like OSCAR, need to be performed to reduce the conservatism from the assumption, or to confirm the results.

Corrosion

- The components manufacture process could have impact on the cooling channels wetted surface quality and hence the corrosion behavior. The current blanket series production with CuCrZr wetted surface reduces build-up of the unexpected oxide layer and roughness of < 1.6 µm.

- The manufacturing route of some blanket components consists of high temperature processes [36]. For the series production, these thermal cycles are undertaken in commercially available ovens, which reduces the progressive build-up of and bonded copper rich flakes within the CuCrZr channels (see figures below) [37].

- For the ITER blanket system, deep gun drilling is extensively used to form the internal cooling channels in SS and CuCrZr [35]. A target CuCrZr surface roughness of < is required for those exposed CuCrZr wetted surfaces. The qualification from ITER supplier shows that this requirement can be achieved [35].



Figure: Manufactured ITER blanket [36-37]



Figure: ITER Blanket CuCrZr high quality wetted surface [36-37]